A molecular link from PAMP perception to a MAPK cascade associated with tomato disease resistance

Sessa, G. Tel Aviv University
Martin, G.B. Boyce Thompson Institute NY

Project award year: 2012
Three year research project

ABSTRACT

The research problem: The detection of pathogen-associated molecular patterns (PAMPs) by plant pattern recognition receptors (PRRs) is a key mechanism by which plants activate an effective immune response against pathogen attack. MAPK cascades are important signaling components downstream of PRRs that transduce the PAMP signal to activate various defense responses. Preliminary experiments suggested that the receptor-like cytoplasmic kinase (RLCK) Mai5 plays a positive role in pattern-triggered immunity (PTI) and interacts with the MAPKKK M3Kε. We thus hypothesized that Mai5, as other RLCKs, functions as a component PRR complexes and acts as a molecular link between PAMP perception and activation of MAPK cascades.

Original goals: The central goal of this research was to investigate the molecular mechanisms by which Mai5 and M3Kε regulate plant immunity. Specific objectives were to: **1.** Determine the spectrum of PAMPs whose perception is transmitted by M3Kε; **2.** Identify plant proteins that act downstream of M3Kε to mediate PTI; **3.** Investigate how and where Mai5 interacts with M3Kε in the plant cell; **4.** Examine the mechanism by which Mai5 contributes to PTI.

Changes in research directions: We did not find convincing evidence for the involvement of M3Kε in PTI signaling and substituted objectives 1 and 3 with research activities aimed at the analysis of transcriptomic profiles of tomato plants during the onset of plant immunity, isolation of the novel tomato PRR FLS3, and investigation of the involvement of the RLCK BSKs in PTI.

Main achievements during this research program are in the following major areas:

1. Functional characterization of Mai5. The function of Mai5 in PTI signaling was demonstrated by testing the effect of silencing the *Mai5* gene by virus-induced gene silencing (VIGS) experiments and in cell death assays. Domains of Mai5 that interact with MAPKKKs and subcellular localization of Mai5 were analyzed in detail.

2. Analysis of transcriptional profiles during the tomato immune responses to *Pseudomonas syringae* (Pombo et al., 2014). We identified tomato genes whose expression is induced specifically in PTI or in effector-triggered immunity (ETI). Thirty ETI-specific genes were examined by VIGS for their involvement in immunity and the MAPKKK EPK1, was found to be required for ETI.

3. Dissection of MAP kinase cascades downstream of M3Kε (Oh et al., 2013; Teper et al., 2015). We identified genes that encode positive (SGT and EDS1) and negative (WRKY1 and WRKY2) regulators of the ETI-associated cell death mediated by M3Kε. In addition, the MKK2 MAPKK, which acts downstream of M3Kε, was found to interact with the MPK3 MAPK and specific MPK3 amino acids involved interaction were identified and found to be required for induction of cell death. We also identified 5 type III effectors of the bacterial pathogen *Xanthomonas euvesicatoria* that inhibited cell death induced by components of ETI-associated MAP kinase cascades.

4. Isolation of the tomato PRR FLS3 (Hind et al., submitted). FLS3, a novel PRR of the LRR-RLK family that specifically recognizes the flagellin epitope flgII-28 was isolated. FLS3 was shown to bind flgII-28, to require kinase activity for function, to act in concert with BAK1, and to enhance disease resistance to *Pseudomonas syringae*.

5. Functional analysis of RLCKs of the brassinosteroid signaling kinase (BSK) family. Arabidopsis and tomato BSKs were found to interact with PRRs. In addition, certain Arabidospsis BSK mutants were found to be impaired in PAMP-induced resistance to *Pseudomonas syringae*.

Scientific and agricultural significance: Our research activities discovered and characterized new molecular components of signaling pathways mediating recognition of invading pathogens and activation of immune responses against them. Increased understanding of molecular mechanisms of immunity will allow them to be manipulated by both molecular breeding and genetic engineering to produce plants with enhanced natural defense against disease.

Summary Sheet

PubType	IS only	Joint	US only
Book Chapter	0	0	1
Reviewed	0	1	2
Submitted	0	0	1

CONTRIBUTION OF COLLABORATION

The achievements described in this report are the result of an active and synergistic collaboration between the Israeli and the American laboratories. Between the two labs there was a constant exchange of resources and expertise during the entire course of the project. VIGS vectors and procedures were developed and calibrated at BTI, and transferred to the TAU group to perform experiments related to the identification of signaling components that act downstream of MAPKKKε and are involved in ETI against *Xanthomonas* bacteria. Assays of cell death induced by overexpression of components of MAP kinase cascades were developed at BTI and employed at TAU to identify *Xanthomonas* type III effectors that inhibit immunity-associated cell death. Mai5 functional studies were carried out at BTI while determination of Mai5 subcellular localization was performed at TAU. Transcriptional profiling of gene expression during immunity and isolation of FLS3 were performed at BTI, while studies on the FLS3-BSKs interactions and BSK functional analysis were carried out at TAU. The PIs reviewed progress and future plans during a visit of Prof. Sessa to BTI (April 2013) and in frequent skype video calls.

ACHIEVEMENTS

1. Functional characterization of Mai5 (manuscript in preparation).

In protein-protein interaction studies, we defined the domains of M3Kε and M3Kα that are required for their interaction with Mai5. The contribution of Mai5 to pattern-triggered immunity (PTI) was analyzed by silencing the *Mai5* gene in *N. benthamiana* plants. Virus-induced gene silencing (VIGS) of *Mai5* compromised the plant response to flg22, as indicated by reduced production of ROS. Furthermore, VIGS of *Mai5* compromised PTI in cell death suppression assays involving pretreatment with non-pathogenic *Pseudomonas fluorescens* bacteria followed by inoculation with a virulent *Pst* strain. Finally, subcellular localization analysis demonstrated association of Mai5 with the plasma membrane.

2. Analysis of transcriptional profiles during the tomato immune responses to *Pseudomonas syringae* bacteria (Pombo et al., 2014).

A high-throughput RNA sequencing analysis of immune responses in tomato plants challenged by *Pseudomonas syringae* pv. *tomato* identified genes whose expression changes specifically during pattern-triggered or effector-triggered immunity (PTI or ETI). We then developed reporter genes for each of these responses. Virus-induced gene silencing of 30 of the effector-triggered immunity-specific genes identified Epk which encodes a predicted protein kinase from a family previously unknown to be involved in immunity. Knocked-down expression of Epk1 compromised ETI triggered by three bacterial effectors but not by effectors from non-bacterial pathogens. Epistasis experiments indicated that Epk1 acts upstream of ETI-associated MAP kinase signaling.

3. Dissection of MAP kinase cascades downstream of M3Kε (Oh et al., 2013; Teper et al., 2015).

We tested the effect of silencing immunity-associated genes on M3Kε-induced cell death. The *SGT1* gene was required for M3Kε-induced cell death, while *EDS1* reduced this phenotype. Conversely, silencing of *WRKY1* and *WRKY2* accelerated the M3Kε-induced cell death suggesting that they are negative regulators of M3Kε-mediated signaling.

We further investigated the role of MKK2, which acts downstream of M3Kε, in elicitation of cell death. *In vivo* assays revealed that MKK2 interacted with the downstream MAPK SlMPK3 and two conserved leucines of its N-terminal MAPK docking site (D-site) were required for the interaction with SlMPK3 and cell death elicitation. This suggests that the D-site play a critical role in regulation of signal transfer to the downstream MAP kinase by participating in the MAPKK-MAPK physical interaction.

We examined the ability of 33 *Xanthomonas* effectors to inhibit cell death induced by overexpression of components of immunity-associated MAPK cascades in *Nicotiana benthamiana* plants. Five effectors inhibited cell death induced by overexpression of MAPKKKα and MEK2, but not of MAP3Kε. In addition, expression of AvrBs1 in yeast suppressed activation of the high osmolarity glycerol MAPK pathway, suggesting that the target of this effector is conserved in eukaryotic organisms. These results indicate that *Xanthomonas* employs several type III effectors to suppress immunity-associated cell death mediated by MAPK cascades.

4. Identification of FLS3, a novel pattern recognition receptor (PRR) that specifically recognizes flgII-28 (Hind et al., submitted). A screen of tomato wild species identified natural variation in the response to the flgII-28 flagellin epitope. By exploiting this variation and using a mapping-by-sequencing approach, we cloned the *Flagellin-sensing 3* (*FLS3*) gene encoding the flgII-28 receptor. FLS3 is a PRR of the leucine-rich-repeat receptor-like kinase (LRR-RLK) type and its transient expression in the insensitive tomato variety Yellow Pear conferred sensitivity to flgII-28, and enhanced immune responses and disease resistance. Photo-affinity labeling demonstrated specific binding of flgII-28 by FLS3 representing a receptor-ligand interaction. Point mutations that were anticipated to abolish kinase activity impaired the signaling ability of FLS3. Finally, FLS3 signaling required the co-receptor BAK1 and was suppressed by the bacterial effectors AvrPto and AvrPtoB.

5. Functional analysis of Arabidopsis RLCKs of the brassinosteroid signaling kinase (BSK) family. Arabidopsis BSK5 was used as a bait to screen a yeast two-hybrid (Y2H) cDNA library. Of the 99 BSK5 interactors identified, 45 were RLKs and among them a large group of known or putative PRRs, and PRR-associated proteins.

In tomato, BSK family members were tested in a yeast two-hybrid (Y2H) system for their interaction with the kinase domain of the tomato PRRs FLS3, FLS2 and Bti9. BSK830 interacted with all three PRRs. By using a split-luciferase complementation assay (SLCA), we confirmed that BSK830 interacted *in planta* with full-length FLS3, FLS2 and Bti9, but not with the Pto kinase.

BSK7 and BSK8 are the closest Arabidopsis homologs of tomato BSK830. The involvement of BSK7 and BSK8 in PTI was tested in a pathogen infection assay with Arabidopsis *bsk7* and *bsk8* T-DNA insertion mutants and wild-type plants pretreated with a PAMP (pep1 and flg22 for *bsk7* and *bsk8* mutants, respectively). Growth of *Pst* in PAMP-pretreated wild-type plants was significantly lower than in water-treated plants, while it was similar in PAMP- and water-pretreated *bsk7* and *bsk8* mutants, indicating that the mutants lost PAMP-induced resistance to *Pst*.

CHANGES TO THE ORIGINAL RESEARCH PLAN

Preliminary experiments suggested that the receptor-like cytoplasmic kinase (RLCK) Mai5 plays a positive role in pattern-triggered immunity and interacts with the MAPKKK M3Kε. Based on these data, we hypothesized that Mai5, as other RLCKs, functions as a component of pathogen recognition receptor (PRR) complexes and acts as a molecular link between PAMP perception and activation of MAPK cascades. However, because during the first year of research we were unable to confirm the involvement of M3Kε in PTI signaling, we were not able to investigate what is the spectrum of PAMPs whose perception is transmitted by M3Kε (objective 1) and what are the plant proteins that act downstream of M3Kε to mediate PTI (objective 2). Instead, we investigated signaling pathways that originate from M3Kε to mediate ETI, analyzed transcriptomic profiles of tomato plants during the onset of PTI and ETI, isolated the tomato PRR FLS3 that specifically recognizes the bacterial PAMP flgII-28, and analyzed the involvement in PTI of Arabidopsis and tomato RLCKs that are members of the brassinosteroid signaling kinase (BSK) family.

Publications for Project IS-4510-12C

Status	Type	Authors	Title	Journal	Volume: Pages	Year	Country
Published	Book Chapter	*Martin, G.B.*	Suppression and activation of the plant immune system by Pseudomonas syringae effectors AvrPto and AvrPtoB.	***In Martin F. and Kamoun S. Editors, Effectors in Plant-Microbe Interactions. Wiley-Blackwell, a John Wiley & Sons Inc. Publication.***	: 123-154	***2012***	US only
Published	Reviewed	*Teper, D., S. Sunitha, G. B. Martin, G. Sessa*	Five Xanthomonas type III effectors suppress cell death induced by components of immunity-associated MAP kinase cascades	***Plant Signal. Behav.***	10 : e1064573	***2015***	Joint
Submitted	Reviewed	*Hind S.R., Strickler S.R., Boyle P.C., Bao Z., O'Doherty I.M., Baccile J.A., Dunham, D.M., Viox, E.G., Clarke C.R., Vinatzer B.A., Schroeder F.C. and Martin G.B.*	Tomato receptor FLAGELLIN-SENSING 3 activates immune signaling		:		US only
Published	Reviewed	*Oh C-S., Hwang J., Choi M-S., Kang B-C. and Martin G.B.*	Two leucines in the N-terminal MAPK-docking site of tomato SlMKK2 are critical for interaction with a downstream MAPK to elicit programmed cell death associated with plant immunity.	***FEBS Lett.***	587 : 1460-1465	***2013***	US only
Published	Reviewed	*Pombo M.A., Zheng Y., Fernandez-Pozo N., Dunham D.M., Fei Z. and Martin G.B.*	Transcriptomic analysis reveals tomato genes whose expression is induced specifically during effector-triggered immunity and identifies the Epk1 protein kinase which is required for the host response to three bacterial effector proteins.	***Genome Biol.***	15 : 492	***2014***	US only

APPENDIX

DATA NOT INCLUDED IN PUBLISHED MANUSCRIPTS

1. Characterization of the interaction of Mai5 with MAP3Kε and MAP3Kα.

In previous studies, we observed an interaction between Mai5 and the MAP3Ks MP3Kε and MAP3Kα. These interactions were characterized further testing the ability of Mai5 to interact with truncated forms of MAP3Kε and MAP3Kα in a yeast two-hybrid system. The kinase domain of MAP3Kα was found to be sufficient for interaction with Mai5 (Fig. 1). In contrast, Mai5 interacted with the full-length MAP3Kε protein but not with truncated forms, raising the possibility that Mai5 interacts with a domain spanning the truncation points or possibly with two physically separated domains of MAP3Kε (Fig. 2). We also obtained additional evidence that the interaction of Mai5 with MAP3Kα and MAP3Kε is specific, as Mai5 did not interact with three other unrelated MAPKKKs (data not shown).

2. Mai5 localizes to the plasma membrane.

We developed a 35S:Mai5-YFP construct and showed that when it is transiently expressed in leaves of *Nicotiana benthamiana* the expected size fusion protein is produced (Fig. 3A). This construct was used for subcellular localization experiments demonstrating that the Mai5 protein is associated with the plasma membrane (Fig. 3B)

3. Involvement of Mai5 in PAMP-triggered immunity (PTI).

The contribution of Mai5 to PTI was analyzed by silencing the corresponding gene in *N. benthamiana* plants and testing the plant response to flg22, a well-characterized PAMP. Virus-induced gene silencing (VIGS) of the *Mai5* gene (or *FlS2* encoding the flg22 receptor, as a positive control) compromised the response of the silenced plants to flg22, as indicated by reduced production of reactive oxygen species (ROS) (Fig. 5). This finding suggests that Mai5 acts downstream of FlS2 in a PTI pathway leading to ROS production. Furthermore, VIGS of *Mai5* (or *FLS2*) also compromised PTI in a leaf-based cell death suppression assay using either *P. syringae* pv. *tomato* DC3000 or a derivative of this strain DC3000*ΔhopQ1-1* as a challenger (Fig. 5). Finally, VIGS of *Mai5* (or *FLS2*) compromised PTI in a whole

plant-based assay involving pre-treatment with *P. fluorescens* followed by inoculation with DC3000*ΔhopQ1-1* (Fig. 6).

4. Identification of plant proteins that act downstream of MAP3Kε in ETI signaling.

To identify plant proteins that act downstream of MAP3Kε, we silenced a group of genes encoding proteins that were previously shown to be part of signaling pathways activated by resistance proteins and tested the effect of their silencing on MAP3Kε-induced cell death. In these experiments, we found that SGT1 was required for MAP3Kε-induced cell death, while EDS1 reduced this phenotype (Fig. 7). Conversely, WRKY1 and WRKY2 accelerated the MAP3Kε-induced cell death suggesting that they act as negative regulators of MAP3Kε-mediated signaling.

5. Analysis of molecular interaction and functional characteristics of Arabidopsis and tomato BSKs.

There are 12 and 7 BSK family members in Arabidopsis and tomato, respectively. To identify interacting partners, BSK5 was used as a bait to screen a yeast two-hybrid (Y2H) cDNA library. Of the 99 BSK5 interactors identified, 45 were RLKs and among them a large group of known or putative PRRs, and PRR-associated proteins (data not shown). In tomato, the seven BSK family members were tested in a yeast two-hybrid (Y2H) system for their interaction with the kinase domain of the tomato PRRs FLS3, FLS2 and Bti9. BSK830, but not other tomato BSKs, interacted with all three PRRs (Fig. 8A, data shown for BSK830). By using a split-luciferase complementation assay (SLCA), we confirmed that BSK830 interacted *in planta* with full-length FLS3, FLS2 and Bti9, but not with the Pto kinase (Fig. 8B).

BSK7 and BSK8 are the closest Arabidopsis homologs of tomato BSK830. The involvement of BSK7 and BSK8 in PTI was tested in a pathogen infection assay with Arabidopsis *bsk7* and *bsk8* T-DNA insertion mutants and wild-type plants pretreated with a PAMP (pep1 and flg22 for *bsk7* and *bsk8* mutants, respectively). Growth of *Pst* in PAMP-pretreated wild-type plants was significantly lower than in water-treated plants, while it was similar in PAMP- and water-pretreated *bsk7* and *bsk8* mutants (Fig. 5A and 5B), indicating that the mutants lost PAMP-induced resistance to *Pst*.

FIGURES

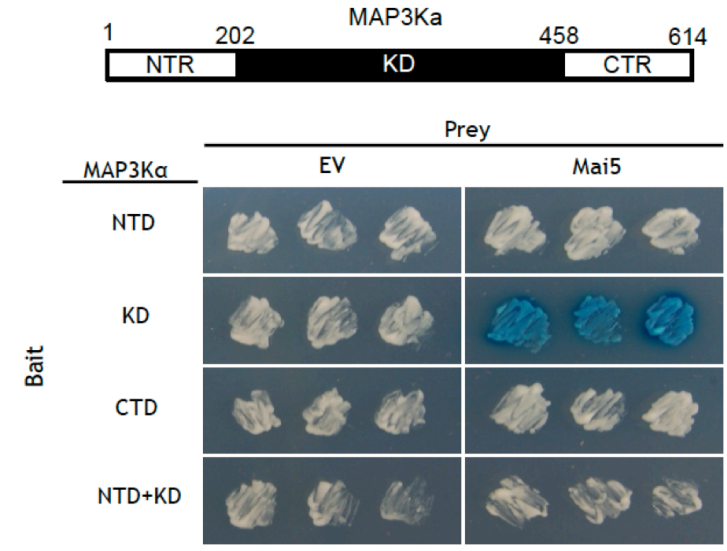

Figure 1. The kinase domain of MAP3Kα interacts with Mai5 in a yeast two-hybrid system. Truncated forms of MAP3Kα were expressed from the pEG202 bait vector, while Mai5 was in the pJG4-5 prey vector. Yeast were transformed with the indicated bait and prey combinations and grown in the presence of x-gal. Blue patches indicate positive interactions while the white color indicates no interaction. NTD, N-terminal domain; KD, kinase domain; CTD, C-terminal domain.

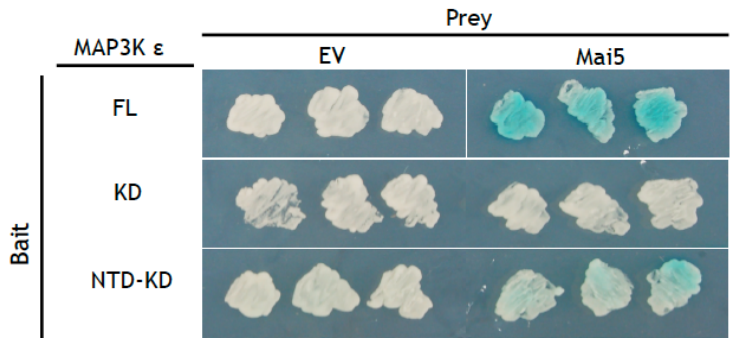

Figure 2. Mai5 interacts with the full-length MAP3Kε but not with truncated forms in a yeast two-hybrid system. Full length or truncated forms of MAP3Ke were expressed from the pEG202 bait vector, while Mai5 was in the pJG4-5 prey vector. Yeast were transformed with the indicated bait and prey combinations and grown in the presence of x-gal. Blue patches indicate positive interactions while the white color indicates no interaction. FL, Full length; NTD, N-terminal domain; KD, kinase domain.

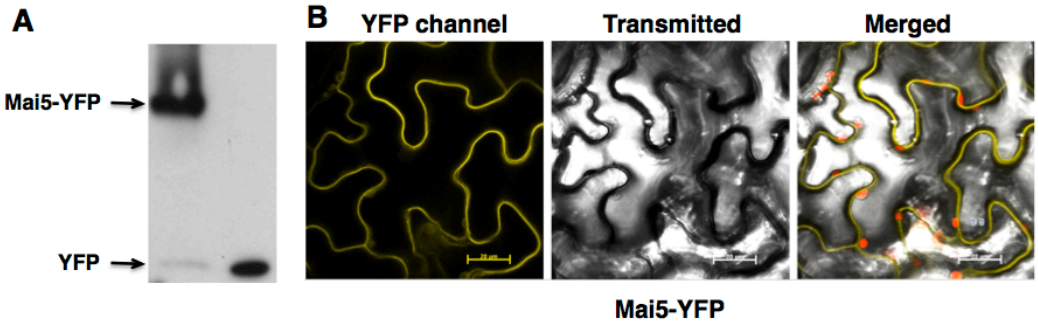

Figure 3. Mai5 is localized to the plant cell periphery in leaf epidermal cells. *Nicotiana benthamiana* leaves were infiltrated with an *Agrobacterium* strain expressing a Mai5-YFP fusion driven by the CaMV 35S promoter. A. Western blot analysis B. Fluorescence was visualized in epidermal leaf cells using a confocal microscope 48 hours after *Agrobacterium* infiltration.

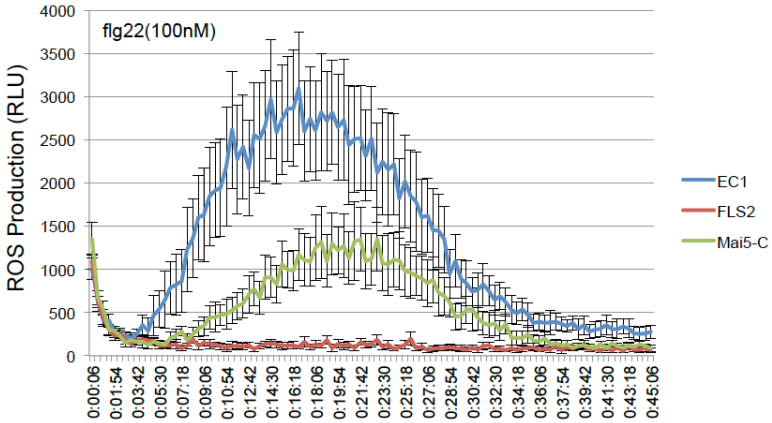

Figure 4. Silencing of Mai5 reduces production of reactive oxygen species (ROS). *N. benthamiana* plants silenced for *Mai5* or *FLS2* and non-silenced (EC1) plants were treated with flg22 (100 nM) and monitored for released of ROS during 45 min.

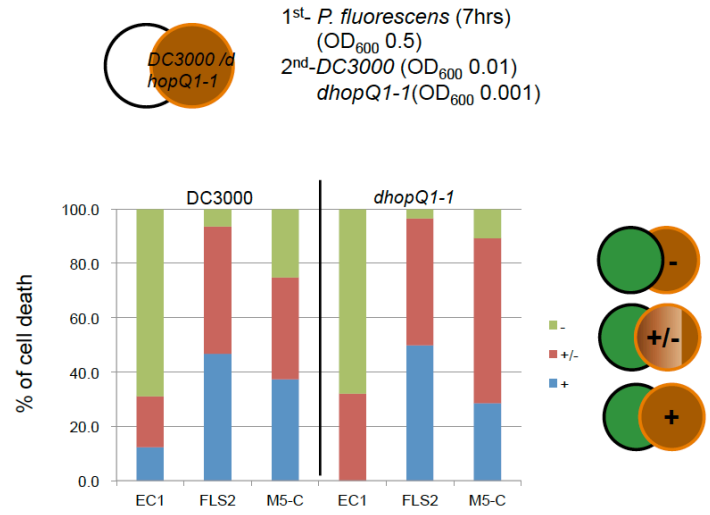

Figure 5. Silencing of Mai5 compromises PTI in a leaf-based cell death suppression assay. *N. benthamiana* plants silenced for *Mai5* or *FLS2* and non-silenced plants (EC1) were first syringe-infiltrated with non-pathogenic *P. fluorescens* (*Pf*) and after 7 hours were infiltrated with cell-death inducing *Pseudomonas syringae* pv. *tomato* DC3000 or its derivative DC3000*ΔhopQ1-1*. DC3000 was infiltrated such that it partially overlapped the *Pf* area. Cell death was recorded 5 days after *Pf* infiltration and cell death in the overlapping area was scored as unaffected, partially or fully compromised.

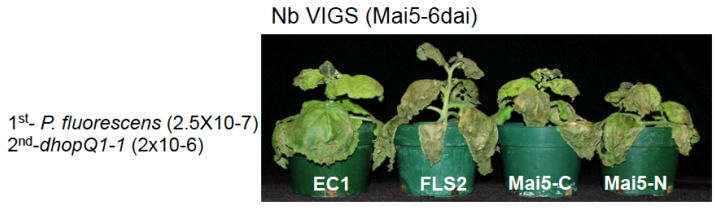

Figure 6. Silencing of Mai5 compromises PTI in a whole plant-based assay. *N. benthamiana* plants silenced for *Mai5* (with a gene fragment corresponding to the N- or C- terminal part of the protein) or *FLS2* and non-silenced plants (EC1) were first syringe-infiltrated with non-pathogenic *P. fluorescens* (*Pf*) and then infiltrated with cell-death inducing *Pseudomonas syringae* pv. *tomato* DC3000*ΔhopQ1-1*. Plants were photographed 6 days after *Pf* infiltration.

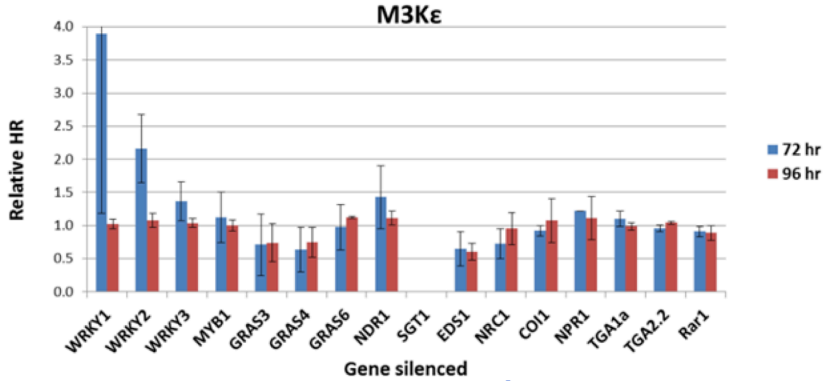

Figure 7. WRKY1, WRKY2 and SGT1 act downstream of MAP3Kε. *N. benthamiana* plants silenced for the indicated genes were infiltrated with *Agrobacterium* carrying a plasmid for the estradiol-inducible expression of MAP3Kε. The extent of cell death induced by MAP3Kε in the silenced plants was quantified at 72 and 96 hours after estradiol application relative to non-silenced plants.

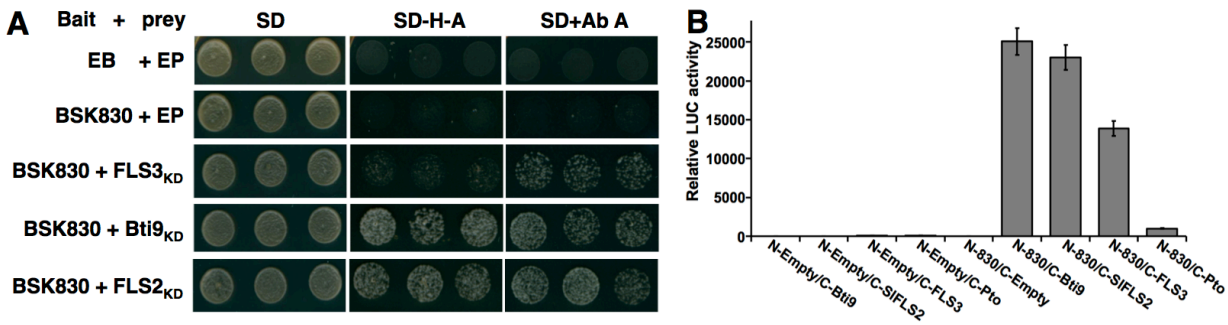

Fig. 8. BSK830 specifically interacts with PRRs in yeast and *in planta*. A, Yeast expressing BSK830 as bait and the kinase domain of the indicated proteins as prey were grown on synthetically defined medium (SD), SD lacking histidine and adenine (SD-H-A), or SD supplemented with Aureobasidin A (SD+AbA). EB, empty bait; EP, empty prey. **B,** *N. benthamiana* leaves were infiltrated with *Agrobacterium* for the expression of the indicated proteins fused to the N-terminal or C-terminal half of the luciferase protein (N- or C-) or an empty vector. Luminescence was measured from extracts of leaf samples. Bars represent averages of three technical repeats ±SD.

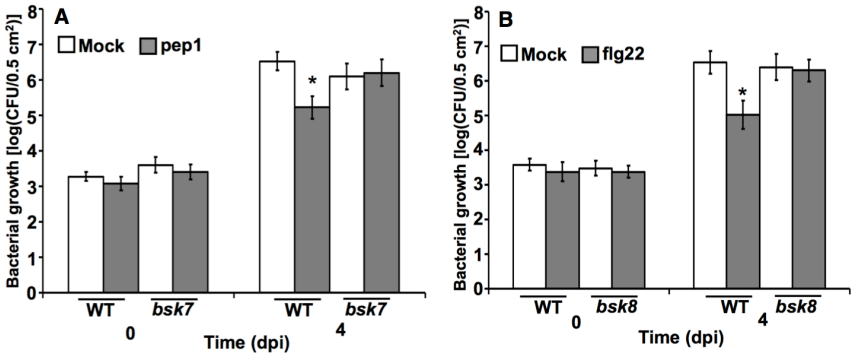

Fig. 5. Arabidopsis *bsk7* and *bsk8* mutants are impaired in PAMP-induced resistance. Wild-type, *bsk7* and *bsk8* mutant plants were treated with a PAMP (pep1 and flg22 for *bsk7* and *bsk8*, respectively) or water, and 24 h later inoculated with *Pst* ($1x10^5$ CFU/ml). Bacterial growth was measured at 0 and 4 days post-inoculation (dpi). Data are the averages of 3 independent experiments ±SD. (*) indicates a significant difference compared to the water control using Student's *t*-test ($P < 0.05$).